

Synchronization properties of logistic maps coupled with random delay times

Arturo C. Martí^{a,*}, Marcelo Ponce^{a,†} and C. Masoller^{a,b‡}

^a*Instituto de Física, Facultad de Ciencias, Universidad de la República, Iguá 4225, Montevideo 11400, Uruguay and
^bDepartament de Física i Enginyeria Nuclear, Universitat Politècnica de Catalunya, Colom 11, E-08222 Terrassa, Spain*

(Dated: February 9, 2020)

We study the synchronization properties of an array of mutually coupled logistic maps, focusing on the influence of the delay times, τ_{ij} , of the interaction between the i th and j th maps. We recently reported [Phys. Rev. Lett. **94**, 134102 (2005)] that if τ_{ij} are random enough the array synchronizes in a spatially homogeneous steady state. Here we study this synchronization behavior by comparing the dynamics of a map of an array of N coupled maps with the dynamics of a map with N self-feedback time-delayed loops. We show that for N large and non-uniform delays the dynamics of a map with self-feedback loops is similar to the dynamics of a map of the array. Several delayed loops stabilize the fixed point; however, the distribution of delays plays a key role: if the delays are all odd a periodic orbit (and not the fixed point) is stabilized. We present a linear stability analysis and apply some mathematical theorems that explain the numerical results.

PACS numbers: 05.45.Xt, 05.65.+b, 05.45.Ra

Keywords: Random delays; synchronization; coupled map arrays; logistic map

I. INTRODUCTION

Coupled map lattices [1] are excellent tools for understanding the mechanisms of emergence of synchrony and collective behavior in complex systems composed of mutually coupled interacting nonlinear units. Cooperative behavior arises in many fields of science and classical examples include the onset of rhythmic activity in the brain, the flashing on and off in unison of populations of fireflies, and the emission of chirps by populations of crickets [2]. Of important practical applications is the synchronization of laser arrays and Josephson junctions. Coupled map lattices have proven to be a useful tool for understanding the emergence of collective behavior because by simplifying the dynamics of an individual units allow the simulation of large ensembles of coupled units.

The effects of time delays arising from the finite propagation time of signals have received considerable attention. Classical examples in physiology and optics are the Mackey-Glass model [3] (that describes anomalies in the regeneration of white blood cells due to the finite time of propagation of chemical substances in the blood) and the Ikeda model [4] (that accounts for the finite velocity of light in optical bistable devices).

Three common consequences of time-delays are multistability, which typically arises for delays longer than the intrinsic oscillation period [5, 6], chaotic dynamics, which arises for strong coupling and/or long delays, and oscillation death, which refers to the existence of stability islands in the parameter space (coupling strength, delay time) where the amplitude of coupled limit-cycle oscillator is zero [7]. It is also well-known that time-delayed feedback can stabilize unstable orbits embedded in chaotic attractors [8] and enhance the coherence of chaotic [9, 10] and stochastic motions [11].

Most studies of delayed coupling have considered uniform delays, i.e., the interactions between the different elements of a network occur all with the same delay time (instantaneous coupling is a particular case of “fixed delay coupling”). Recently, attention has been focused on the influence of distributed (or random) delays. Several authors have reported that non-uniform delays often have a stabilizing effect. Atay et al. [12] studied ensembles of limit-cycle oscillators and showed that distributed delays can enlarge the stability islands where oscillator death occurs. Huber and Tsimring [13] studied networks of globally coupled, noise-activated, bistable elements and found that increasing the non-uniformity of the delays enhanced the stability of the trivial equilibrium. Eurich et al. [14] showed that distributed delays increase the stability of predator-prey systems including two-species systems, food chains, and food webs.

Two of us recently studied the dynamics of an array of logistic maps coupled with randomly distributed delay times [15],

$$x_i(t+1) = f[x_i(t)] + \frac{\epsilon}{N} \sum_{j=1}^N (f[x_j(t - \tau_{ij})] - f[x_i(t)]), \quad (1)$$

where t is a time index, $i = 1, \dots, N$ is a space index, $f(x) = ax(1 - x)$ is the logistic map ($a \in (0, 4]$), ϵ is the coupling strength ($\epsilon \in [0, 1]$) and $\tau_{ij} \geq 0$ is the delay time in the interaction between the i th and j th maps. For τ_{ij} random enough the array synchronizes in the spatially homogeneous nontrivial steady-state, $x_i(t) = x_0$ for all i , with $x_0 = f(x_0)$ (for the logistic map $x_0 = 1 - 1/a$). This synchronization behavior is in contrast with the synchronization with fixed and distant-dependent delays. For fixed delays ($\tau_{ij} = \tau_0 \forall i, j$) the array synchronizes in a spatially homogeneous time-dependent state,

$x_i(t) = x(t) \forall i, t$, where the dynamics of an element of the array is either periodic or chaotic depending on τ_0 [16]. For distant-dependent delays ($\tau_{ij} = k|i - j|$ where k is the inverse of the velocity of transmission of information) a linear, one-dimensional array synchronizes in a state in which the elements of the array evolve along a periodic orbit of the uncoupled map (i.e., $x_i(t)$ is a solution of $x_i(t+1) = f[x_i(t)]$), while the spatial correlation along the array is such that $x_i(t) = x_j(t - \tau_{ij}) \forall i, j$ (i.e., an individual map sees all other maps in his present, current, state) [17].

In [15] the synchronization behavior of an array of logistic maps coupled with random interaction delay times was interpreted as a “discrete time” version of the multiple delay feedback control method recently proposed by Ahlborn and Parlitz [18] for stabilizing steady states. In [18] the fixed point of a dynamical system $\dot{x} = f(x)$ was stabilized with the addition of several feedback terms that satisfy: (i) the feedback terms vanish in the steady state and (ii) the delay times are not an integer multiple of each other (with these conditions the control terms vanish only at the fixed points and not at the periodic orbits). Simulations of a single logistic map with N self-feedback time-delayed loops,

$$x(t+1) = f[x(t)] + \frac{\epsilon}{N} \sum_{j=1}^N f[x(t - \tau_j)] - f[x(t)], \quad (2)$$

show that the inclusion of several terms with different delay times can lead to the stabilization of the fixed point after transients.

The behavior of a single unit often helps understanding the behavior of an ensemble of coupled units, and in particular the “chaos suppression by random delays” in an ensemble of coupled logistic maps can be interpreted in terms of the suppression of chaos and the stabilization of the fixed point in a single logistic map with several delayed self-feedback loops. The aim of this paper is to further investigate this point, by comparing the dynamics of an element x_i of an array of N logistic maps [Eq.(1)] with that of a map with N self-feedback loops [Eq.(2)].

This paper is organized as follows. Section II presents a linear stability analysis of the fixed point solution of Eq.(2) and discusses the stability in the parameter space local nonlinearity, a , coupling strength, ϵ . Section III presents results of numerical simulations that show that for N large and random delays the dynamics of one map with N feedback loops is similar to the dynamics of one map of an array of N coupled maps. Section IV presents a summary and the conclusions.

II. STABILITY ANALYSIS

To analyze the stability of the nontrivial fixed point solution of Eq.[2], $x_0 = f(x_0)$ (for the logistic map $x_0 =$

$1 - 1/a$), we define a new set of variables,

$$y_m(t) = x(t - m), \quad (3)$$

with $m = 0, \dots, M$ and $M = \max(\tau_j)$, that describe the present and past state of the map. We can re-write Eq.(2) in terms of these new variables as:

$$y_m(t+1) = \begin{cases} y_{m-1}(t) & \text{if } m \neq 0, \\ (1 - \epsilon)f[y_0(t)] + \frac{\epsilon}{N} \sum_{i=1}^N f[y_{\tau_i}] & \text{if } m = 0. \end{cases} \quad (4)$$

The fixed-point solution is

$$y_0(t) = x_0; \dots; y_M(t) = x_0. \quad (5)$$

To study the stability of this solution we linearize,

$$\delta y_m(t+1) = \sum_{n=0}^M A_{mn} \delta y_n(t), \quad (6)$$

where

$$A = \begin{pmatrix} (1 - \epsilon)f'(x_0) & \alpha_1 & \alpha_2 & \dots & \alpha_{M-1} & \alpha_M \\ 1 & 0 & 0 & \dots & 0 & 0 \\ 0 & 1 & 0 & \dots & 0 & 0 \\ \vdots & & & & \vdots & \\ 0 & 0 & 0 & \dots & 0 & 0 \\ 0 & 0 & 0 & \dots & 1 & 0 \end{pmatrix}. \quad (7)$$

Here

$$\alpha_n = \frac{\epsilon}{N} \sum_{i=1}^N f'[y_{\tau_i}(t)] \delta_{\tau_i n} = l_n \frac{\epsilon}{N} f'(x_0), \quad (8)$$

where l_n is the number of times the value $\tau = n$ appears in the sequence $\tau_1, \tau_2, \dots, \tau_N$: $\sum_{n=1}^M l_n = N$. For simplicity we assume that $\tau_j \neq 0 \forall j$ (the analysis can be extended to account for instantaneous feedback loops). Notice that some of the α_n coefficients will be zero ($\alpha_n = 0$ if $\tau_i \neq n \forall i$); however, the coefficient corresponding to the maximum delay, $M = \tau_{\max}$, is different from zero and is given by

$$\alpha_M = l_M \frac{\epsilon}{N} f'(x_0). \quad (9)$$

The next step for the derivation of analytic stability conditions is the study the eigenvalues λ_i (with $i = 0 \dots M$) of the matrix A . The Gershgorin theorem [19] states that all eigenvalues of a complex square matrix are located in a set of disks centered at the diagonal elements a_{ii} with radius equal to the sum of the norms of the other elements on the same row:

$$|\lambda_i - a_{ii}| \leq \sum_{j \neq i} |a_{ij}|. \quad (10)$$

For $i \neq 0$ Eq.(10) gives $|\lambda_i| \leq 1$ and for $i = 0$ gives

$$|\lambda_i - (1 - \epsilon)f'(x_0)| \leq \sum_{j=1}^M |\alpha_j| = \epsilon |f'(x_0)|, \quad (11)$$

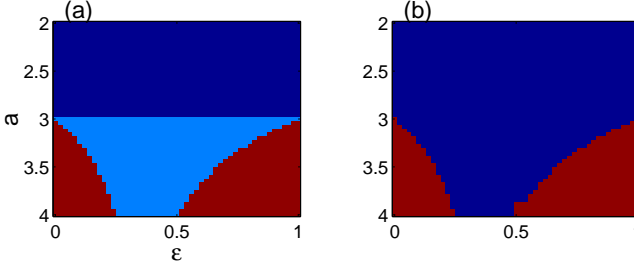


FIG. 1: (a) Analytically calculated stability regions for the logistic map with one delay term ($N = 1$, $\tau_1 = 1$). The stability region defined by Eq. (14) is displayed in black (blue online), the instability regions defined by Eqs. (15) and (21) are displayed in dark grey (red online). (b) Stability regions calculated numerically, by simulation of Eq. (2). The parameter region where the fixed point is stable is displayed in black (blue online).

where we used that $\sum l_j = N$ and $\sum \alpha_j = \epsilon f'(x_0)$. Therefore, the eigenvalues are in the region of the complex plane defined by the two disks:

$$|\lambda| \leq 1 \quad (12)$$

$$|\lambda - (1 - \epsilon)f'(x_0)| \leq \epsilon|f'(x_0)|. \quad (13)$$

From here we can derive a sufficient stability condition and a sufficient instability condition. If the disc of radius $\epsilon|f'(x_0)|$ centered at $(1 - \epsilon)f'(x_0)$ is completely inside the disc radius 1 centered at 0, then all the eigenvalues will have $|\lambda| < 1$. Therefore, a sufficient stability condition is $|(1 - \epsilon)f'(x_0)| + \epsilon|f'(x_0)| < 1$, i.e.,

$$|f'(x_0)| < 1. \quad (14)$$

The stability is trivial because in this case the fixed point of the “solitary map” (the map without feedback loops, $\epsilon = 0$) is stable.

Let us consider the region where $|f'(x_0)| > 1$ (for the logistic map $|f'(x_0)| > 1$ if $a > 3$). In this region we have the following sufficient instability condition. If

$$|(1 - \epsilon)f'(x_0)| - \epsilon|f'(x_0)| > 1, \quad (15)$$

then the disc centered at $(1 - \epsilon)f'(x_0)$ of radius $\epsilon|f'(x_0)|$ is completely outside the disc centered at zero of radius 1, and therefore exists at least one eigenvalue with $|\lambda| \geq 1$.

These regions are displayed in Fig. 1(a) for the logistic map with $N = 1$ and $\tau_1 = 1$. The stability region occurs for $a \leq 3$ while the instability region occurs in the corner of large a and small ϵ (there is a second instability region, in the corner of large a and ϵ which is discussed below). For comparison, we also show in Fig. 1(b) results of numerical simulations of Eq.(2), which agree well with the analytic predictions.

Additional information can be obtained by calculating explicitly the eigenvalues of A as the roots of the charac-

teristic equation

$$\det \begin{pmatrix} (1 - \epsilon)f'(x_0) - \lambda & \alpha_1 & \alpha_2 & \dots & \alpha_{M-1} & \alpha_M \\ 1 & -\lambda & 0 & \dots & 0 & 0 \\ 0 & 1 & -\lambda & \dots & 0 & 0 \\ \vdots & & & & \vdots & \\ 0 & 0 & 0 & \dots & -\lambda & 0 \\ 0 & 0 & 0 & \dots & 1 & -\lambda \end{pmatrix} = 0, \quad (16)$$

that can be written in terms of the determinant of two $M \times M$ matrices:

$$[(1 - \epsilon)f'(x_0) - \lambda] \det C - \det B = 0, \quad (17)$$

where

$$C = \begin{pmatrix} -\lambda & 0 & \dots & 0 & 0 \\ 1 & -\lambda & \dots & 0 & 0 \\ \vdots & & & & \vdots \\ 0 & 0 & \dots & -\lambda & 0 \\ 0 & 0 & \dots & 1 & -\lambda \end{pmatrix} \quad (18)$$

and

$$B = \begin{pmatrix} \alpha_1 & \alpha_2 & \dots & \alpha_{M-1} & \alpha_M \\ 1 & -\lambda & \dots & 0 & 0 \\ \vdots & & & & \vdots \\ 0 & 0 & \dots & -\lambda & 0 \\ 0 & 0 & \dots & 1 & -\lambda \end{pmatrix}. \quad (19)$$

We calculated the determinant of each matrix recursively (details are presented in the appendix) obtaining:

$$\lambda^{M+1} - [(1 - \epsilon)f'(x_0)]\lambda^M - \sum_{j=1}^M \alpha_j \lambda^{M-j} = 0 \quad (20)$$

The roots of Eq.(20) satisfy $\prod_{i=0}^M |\lambda_i| = |\alpha_M|$. Therefore, if

$$|\alpha_M| = |l_M \epsilon f'(x_0)/N| > 1 \quad (21)$$

at least one eigenvalue has $|\lambda| > 1$, i.e., this is an additional (sufficient) instability condition. For $l_M/N = 1$ this condition gives the instability region in the right-bottom corner of Fig. 1(a) (large a and ϵ); for $l_M/N < 1$ this condition is not satisfied in the parameter region of interest ($a \in [0,4]$, $\epsilon \in [0,1]$).

Two special cases are interesting for discussion: all-even and all-odds delays. First, let us show that if the delays are all even (and therefore, M is even), $\lambda = -1$ is a solution of Eq. (20) when $f'(x_0) = -1$, i.e., at the border of the stability region Eq.(14). Substituting $\lambda = -1$ in (20) and taking into account that $M - j$ is even (since in the sum only terms with j even are different from zero) gives

$$-1 - [(1 - \epsilon)f'(x_0)] - \sum_{j=1}^M \alpha_j = 0. \quad (22)$$

Using $\sum_{j=1}^M \alpha_j = \epsilon f'(x_0)$ we obtain $f'(x_0) = -1$. This indicates that in the case of all-even delays there is an eigenvalue $\lambda = -1$ if and only if $a = 3$, regardless of ϵ .

Next, let's see what happens if the delay times are all odd (and therefore, also M is odd). Taking into account that $M - j$ is even (since in the sum only terms with j odd are different from zero) for $\lambda = -1$ Eq. (20) gives

$$1 + [(1 - \epsilon)f'(x_0)] - \sum_{j=1}^M \alpha_j = 0. \quad (23)$$

Using $\sum_{j=1}^M \alpha_j = \epsilon f'(x_0)$ we obtain $f'(x_0) = -1/(1-2\epsilon)$. For the logistic map this gives $a = (3 - 4\epsilon)/(1 - 2\epsilon)$ a condition which is satisfied for $\epsilon \in [0, 1]$ for values of a inside the stability region $a < 3$.

The above analysis allows us to draw some additional conclusions about the stability of the fixed point in the special cases of all-even and all-odd delays. For all-even delays an eigenvalue is real and negative and equal to -1 for $a = 3$. For larger a this eigenvalue can in principle become $\lambda < -1$ rendering the fixed point unstable due to a period-doubling bifurcation. For all-odd delays this is not possible, as $\lambda = -1$ in a parameter region where we know that all eigenvalues must have $|\lambda| \leq 1$.

We verified these predictions by calculating numerically the eigenvalues of A . Figure 2 displays results for all-odd and all-even delays, for varying a while keeping ϵ constant. It can be observed that for all-even delays an eigenvalue crosses the unit circle at $\lambda = -1$ for $a = 3$, while for all-odd delays a pair of complex conjugate eigenvalues cross the unit circle.

III. RESULTS OF SIMULATIONS

In this section we present results of numerical simulations comparing the dynamics of a map with N self-feedback delayed loops, Eq. (2), with the dynamics of a map of an array of N coupled maps, Eq. (1).

Figure 3 displays results for a single map with feedback loops that have all-different delay times ($\tau_j = j \forall j = 1 \dots N$). It can be observed that as N increases the region where the fixed point is stable grows, covering almost all the parameter region $a \in [0, 4]$, $\epsilon \in [0, 1]$, excluding the left-bottom corner (large a , low ϵ) where we found in the previous section that the sufficient instability condition holds [Eq.(15)].

While the above observation of enhanced stability with increasing N is generic to various delay distributions, there is an important exception which is the case of all even delays. In this case the fixed point is stable only in the region defined by the sufficient stability condition, Eq.(14). This is due to the fact that all-even delays stabilize a periodic orbit of the solitary map (as it was discussed in the previous section, the instability of the

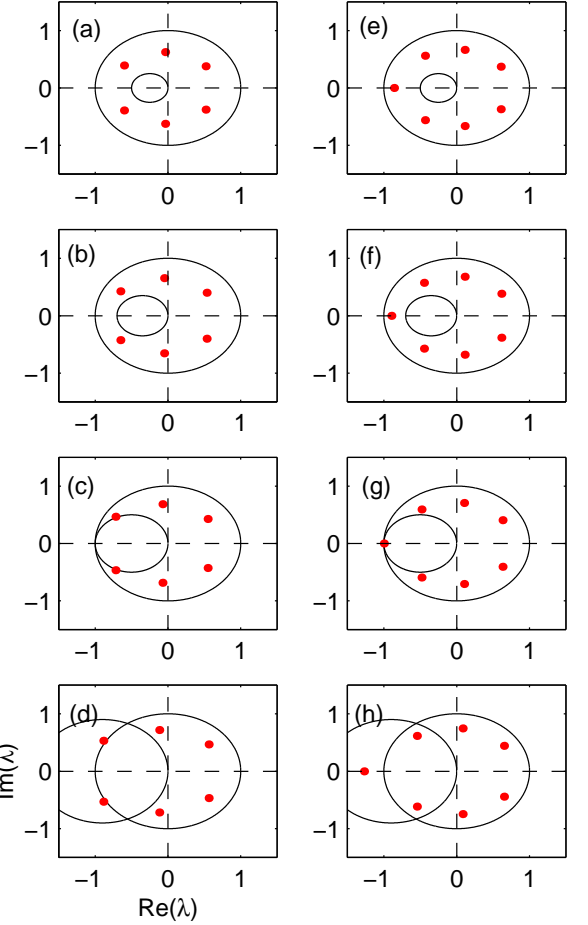


FIG. 2: Eigenvalues in the complex plane for a map with $N = 3$ feedback loops with all-odd delays (left column: $\tau_j = 1, 3, 5$) and all-even delays (right column: $\tau_j = 2, 4, 6$). $\epsilon = 0.5$ and (a), (e) $a = 2.5$; (b), (f) $a = 2.7$; (c), (g) $a = 3.0$ and (d), (h) $a = 3.8$. The circles indicate the Gershgorin disks.

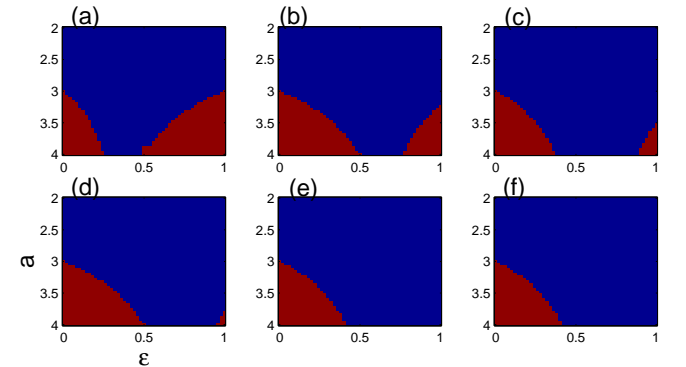


FIG. 3: Numerically calculated stability region of the fixed point solution of a map with N delayed feedback loops. The delays are such that $\tau_j = j$ with $j = 1 \dots N$. (a) $N = 1$, (b) $N = 2$, (c) $N = 3$, (d) $N = 4$, (e) $N = 5$, (f) $N = 6$.

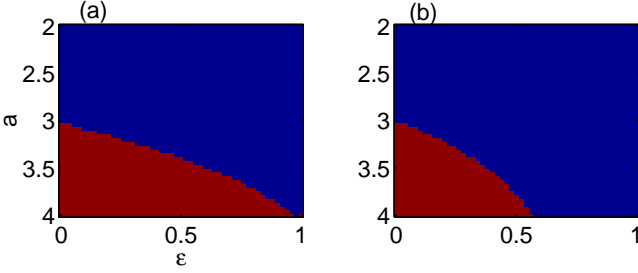


FIG. 4: Numerically calculated stability regions for an array of $N = 5$ (a) and $N = 50$ (b) maps coupled with uniformly distributed delays: $\tau_{ij} \in [1, 10]$.

fixed point arises because one real eigenvalue becomes $\lambda < -1$.

A similar dynamics is observed in an element of an array of N coupled maps [Eq. (1)]. Figure 4 displays the stability region of the homogeneous steady-state solution, $x_i(t) = x_0 \forall i$, for uniformly distributed delays, $\tau_{ij} \in [1, 10]$, and two system sizes: $N = 5$ (a) and $N = 50$ (b) maps. It can be observed that for $N = 50$ the synchronization region is similar to that of the single map with several delayed terms [Fig. 3(f)]. We have also observed (not shown) that in the case of all even delays the homogeneous steady-state is stable only in the region $a \leq 3$, in agreement with the behavior observed in a map with several delayed loops.

Moreover, for N large enough and randomly distributed delays the bifurcations for increasing ϵ of one map of the array and of a map with feedback loops (and with the same delay times) are remarkably similar. Figures 5 (a), (c), (e) display 100 consecutive interactions (after transients die away) of one element, $i = 1$, of an array of $N = 20$ maps vs. ϵ . For comparison, Figs. 5 (b), (d), (f) display 100 consecutive interactions of a map with $N = 20$ feedback loops with the same delay times (in Eq.(2) $\tau_j = \tau_{1j}$ with $j = 1, \dots, 20$). The delays are Gaussian distributed and are “mixed” (even and odd) in Figs. 5(a),(b); all-odd in Figs. 5(c),(d), and all-even in Figs. 5(e),(f). In the case of one map with feedback loops, it can be observed that with “mixed” delays the fixed point is stabilized for increasing ϵ after a period-doubling bifurcation [Fig. 5(b)]. In contrast, with all-odd delays the fixed point is stabilized after a Hopf bifurcation [which occurs at a higher value of ϵ , Fig. 5(d)]. With all-even delays the fixed point is not stable for any ϵ [but the period-two orbit is stable in a certain range of ϵ , Fig. 5(f)]. These results are in agreement with the analysis of the previous section, where we saw that for all-odd delays the fixed point loses stability when a pair of complex eigenvalues cross the unit circle, and for all-even delays the fixed point loses stability when a real eigenvalue crosses the unit circle at $\lambda = -1$. The bifurcation diagrams of the $i = 1$ map of the array display similar

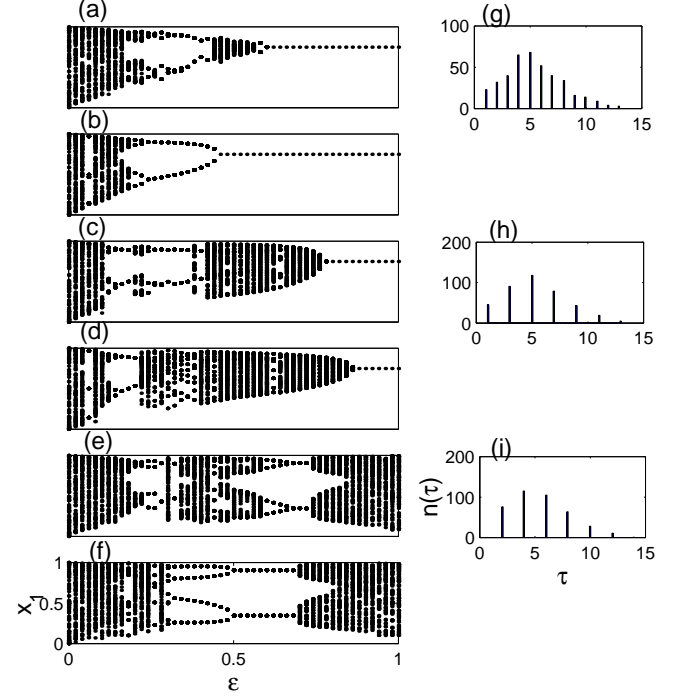


FIG. 5: Bifurcation diagrams for increasing ϵ , $a = 4$ and $N = 20$. (a),(c),(e) One element of an array. (b), (d), (f) One map with delayed loops. In (a),(b) the delays are gaussian distributed, the distribution is shown in (g). In (c), (d) the delays are all-odd gaussian distributed, the distribution is shown in (h). In (e), (f) the delays are all-even gaussian distributed, the distribution is shown in (i).

features: for large ϵ the fixed point is stable in the cases of “mixed” and all-odd delays, while the period-two orbit is stable in a range of ϵ in the case of all-even delays.

III. SUMMARY AND CONCLUSIONS

We investigated the dynamics of mutually coupled logistic maps focusing on the influence of the delay times of the interactions between the maps, and comparing with the dynamics of a map with several time-delayed feedback loops. By using some mathematical tools such as the Gershgorin theorem we derived analytic stability and instability conditions for the fixed point solution of the map with feedback loops. We found that the synchronization properties of the array can be well understood in terms of the dynamics of the map. Specifically, for randomly distributed delay times, if N and ϵ are large enough the fixed-point is stable for both, the map with self-feedback loops and the array. Also, if the delay times are all even, for both, the single map with N delayed loops and the array of N coupled maps, we observed that the stability of the fixed-point is reduced to the “trivial” region ($a \leq 3$) regardless of the coupling strength. The

results presented here provide another example of an ensemble of mutually coupled interacting units, where the understanding of the dynamics of a single unit with self-feedback loops is relevant for the understanding of the macroscopic behavior of the ensemble.

APPENDIX

In this appendix we demonstrate Eq. (20). We start from Eq. (17),

$$[(1 - \epsilon)f'(x_0) - \lambda] \det C - \det B = 0, \quad (24)$$

and calculate the determinant of matrix C recursively:

$$\begin{aligned} \det C &= \det \begin{pmatrix} -\lambda & 0 & 0 & \dots & 0 & 0 \\ 1 & -\lambda & 0 & \dots & 0 & 0 \\ 0 & 1 & -\lambda & \dots & 0 & 0 \\ \vdots & & & & \vdots & \\ 0 & 0 & 0 & \dots & -\lambda & 0 \\ 0 & 0 & 0 & \dots & 1 & -\lambda \end{pmatrix} \\ &= -\lambda \det \begin{pmatrix} -\lambda & 0 & \dots & 0 & 0 \\ 1 & -\lambda & \dots & 0 & 0 \\ \vdots & & & \vdots & \\ 0 & 0 & \dots & -\lambda & 0 \\ 0 & 0 & \dots & 1 & -\lambda \end{pmatrix} \\ &\quad - \det \begin{pmatrix} 0 & 0 & \dots & 0 & 0 \\ 1 & -\lambda & \dots & 0 & 0 \\ \vdots & & & \vdots & \\ 0 & 0 & \dots & -\lambda & 0 \\ 0 & 0 & \dots & 1 & -\lambda \end{pmatrix} \end{aligned} \quad (25)$$

The second determinant is zero because the elements of the first row are all zero. We obtain

$$\det C(M) = -\lambda \det C(M-1) = \dots = (-\lambda)^M. \quad (26)$$

The determinant of matrix B can also be calculated

recursively:

$$\begin{aligned} \det B &= \det \begin{pmatrix} \alpha_1 & \alpha_2 & \alpha_3 & \dots & \alpha_{M-1} & \alpha_M \\ 1 & -\lambda & 0 & \dots & 0 & 0 \\ 0 & 1 & -\lambda & \dots & 0 & 0 \\ \vdots & & & & \vdots & \\ 0 & 0 & 0 & \dots & -\lambda & 0 \\ 0 & 0 & 0 & \dots & 1 & -\lambda \end{pmatrix} \\ &= \alpha_1 \det \begin{pmatrix} -\lambda & 0 & \dots & 0 & 0 \\ 1 & -\lambda & \dots & 0 & 0 \\ \vdots & & & \vdots & \\ 0 & 0 & \dots & -\lambda & 0 \\ 0 & 0 & \dots & 1 & -\lambda \end{pmatrix} \\ &\quad - \det \begin{pmatrix} \alpha_2 & \alpha_3 & \dots & \alpha_{M-1} & \alpha_M \\ 1 & -\lambda & \dots & 0 & 0 \\ \vdots & & & \vdots & \\ 0 & 0 & \dots & -\lambda & 0 \\ 0 & 0 & \dots & 1 & -\lambda \end{pmatrix} \end{aligned} \quad (27)$$

It can be noticed that the first matrix is $C(M-1)$ while the determinant of the second matrix can be calculated recursively,

$$\det B(M) = \alpha_1 \det C(M-1) - \det B(M-1), \quad (28)$$

where

$$B(M-1) = \begin{pmatrix} \alpha_2 & \dots & \alpha_{M-1} & \alpha_M \\ \vdots & & & \vdots \\ 0 & \dots & -\lambda & 0 \\ 0 & \dots & 1 & -\lambda \end{pmatrix}. \quad (29)$$

Substituting in (24)

$$[(1 - \epsilon)f'(x_0) - \lambda] \det C(M) - [\alpha_1 \det C(M-1) - \alpha_2 \det C(M-2) + \det B(M-2)] = 0 \quad (30)$$

Using Eqs.(26) and(28) we obtain

$$[(1 - \epsilon)f'(x_0) - \lambda](-\lambda)^M - \alpha_1(-\lambda)^{M-1} + \alpha_2(-\lambda)^{M-2} - \dots = 0 \quad (31)$$

which gives

$$\begin{aligned} &(-\lambda)^{M+1} + [(1 - \epsilon)f'(x_0)](-\lambda)^M \\ &+ \sum_{j=1}^M (-1)^j \alpha_j (-\lambda)^{M-j} = 0, \end{aligned} \quad (32)$$

that can be simplified to

$$-\lambda^{M+1} + [(1 - \epsilon)f'(x_0)]\lambda^M + \sum_{j=1}^M \alpha_j \lambda^{M-j} = 0. \quad (33)$$

* Electronic address: marti@fisica.edu.uy

[†] Electronic address: mponce@fisica.edu.uy

[‡] Electronic address: cris@fisica.edu.uy

[1] K. Kaneko, Phys. Rev. Lett. **63**, 219 (1989); K. Kaneko, I. Tsuda, *Complex Systems: Chaos and Beyond, A Constructive Approach with Applications in Life Sciences* (Springer-Verlag, Berlin, Heidelberg, New York, 2000).

[2] A.S. Pikovsky, M.G. Rosenblum, and J. Kurths, *Synchronization-A Universal Concept in Nonlinear Sciences* (Cambridge University Press, Cambridge, England, 2001).

[3] M. C. Mackey and L. Glass, Science **197**, 287 (1977).

[4] K. Ikeda, Opt. Commun. **30**, 257 (1979).

[5] J. Foss, A. Longtin, B. Mensour, and J. Milton, Phys. Rev. Lett. **76**, 708 (1996).

[6] M. K. S. Yeung and S. H. Strogatz, Phys. Rev. Lett. **62**, 648 (1999).

[7] D. V. Ramana Reddy, A. Sen, and G. L. Johnston, Phys. Rev. Lett. **80**, 5109 (1998).

[8] K. Pyragas, Phys.Lett.A **170**, 421 (1992).

[9] D. Goldobin et al., Phys. Rev. E **67**, 061119 (2003).

[10] S. Boccaletti et al., Phys. Rev. E **69**, 066211 (2004).

[11] N. B. Janson et al., Phys. Rev. Lett. **93**, 010601 (2004); A. G. Balanov et al., Physica D **199**, 1 (2004).

[12] F. M. Atay, Phys. Rev. Lett. **91**, 094101 (2003).

[13] D. Huber and L. S. Tsimring, Phys. Rev. E **71**, 036150 (2005).

[14] C. W. Eurich, A. Thiel, and L. Fahse, Phys. Rev. Lett. **94**, 158104 (2005).

[15] C. Masoller and A. C. Marti, Phys. Rev. Lett. **94**, 134102 (2005).

[16] F. M. Atay et al., Phys. Rev. Lett. **92**, 144101 (2004).

[17] A. C. Marti and C. Masoller, Phys. Rev. E **67**, 056219 (2003); C. Masoller, A. C. Marti and D. H. Zanette, Physica A **325**, 186 (2003); A. C. Marti and C. Masoller, Physica A **342**, 344 (2004).

[18] A. Ahlborn and U. Parlitz, Phys. Rev. Lett. **93**, 264101 (2004).

[19] J. Stoer and R. Burlisch, *Introduction to Numerical Analysis* (Springer, Berlin, 1992); P.A. Horn and C.R. Jonhson, *Matrix Analysis* (Cambridge University Press, New York, 1985). For a recent application of the Gershgorin theorem see: M. Timme et al., Phys. Rev. Lett. **92**, 074101 (2004).